

Review

Biocompatible Hydrotalcite Nanohybrids for Medical Functions

Wenji Jin ^{1,2}, Dongki Lee ¹, Yukwon Jeon ^{3,*} and Dae-Hwan Park ^{1,*}

¹ Department of Nano Materials Science and Engineering, Kyungnam University, Changwon 51767, Gyeongsangnamdo, Korea; jinwenji7@163.com (W.J.); dlehdrl1229@gmail.com (D.L.)

² College of Chemistry and Environmental Engineering, Jiujiang University, Jiujiang 332005, Jiangxi, China

³ Department of Environmental Engineering, Yonsei University, Wonju 26493, Gangwondo, Korea

* Correspondence: ykjeon@yonsei.ac.kr (Y.J.); dhpark@kyungnam.ac.kr (D.-H.P.);
Tel.: +82-55-249-6432 (D.-H.P.)

Received: 31 December 2019; Accepted: 6 February 2020; Published: 14 February 2020



Abstract: Biocompatible hydrotalcite nanohybrids, i.e., layered double hydroxide (LDH) based nanohybrids have attracted significant attention for biomedical functions. Benefiting from good biocompatibility, tailored drug incorporation, high drug loading capacity, targeted cellular delivery and natural pH-responsive biodegradability, hydrotalcite nanohybrids have shown great potential in drug/gene delivery, cancer therapy and bio-imaging. This review aims to summarize recent progress of hydrotalcite nanohybrids, including the history of the hydrotalcite-like compounds for application in the medical field, synthesis, functionalization, physicochemical properties, cytotoxicity, cellular uptake mechanism, as well as their related applications in biomedicine. The potential and challenges will also be discussed for further development of LDHs both as drug delivery carriers and diagnostic agents.

Keywords: hydrotalcite; nanohybrids; layered double hydroxide; biomedical; therapy; bio-imaging

1. Introduction

Layered double hydroxides (LDHs) are also referred to as hydrotalcite-like anionic clay minerals, since their crystal and chemistry structure are similar to those of the natural mineral, hydrotalcite, which has a chemical composition fixed as $Mg_6Al_2(OH)_{16}CO_3 \cdot 4H_2O$ with $Mg^{2+}:Al^{3+}$ ratio of 3:1 and CO_3^{2-} for balancing interlayer anion [1]. Hydrotalcite has been used for many decades as an antacid and anti-pepsin agent for the earliest application in medical field [2,3]. The new developments from the late 1990s in the area of nanotechnology have resulted in successful synthesis through nanoengineering, and it has led to a paradigm shift to a whole new field for nanomedical applications [4–13].

The synthetic LDH in the form of a natural mineral, hydrotalcite, has already been commercialized as the antacid and anti-pepsin agent with the drug product name of “Talcid[®]” by Bayer, a European biopharmaceutical company [3]. Hydrotalcite, one of the layered lattice antacids, is the active ingredient in the proven layered antacid, Talcid[®]. It is effective for the symptomatic treatment of acid-related stomach problems and heartburn. The original mineral was first discovered by geologist Carl Hochstetter in Sweden in 1842 and he referred to it as “hydrotalcite”. It has the excellent property of gastric acid-binding. Since 1972, the hydrotalcite mineral has been synthesized and found to be successful when used in acid-related stomach complaints such as acid binders, for example Talcid[®].

The components of hydrotalcite form a stable, sandwich-like layered structure and release amounts from the layered grid, depending on the pH value. Hydrotalcite has the characteristic of even being able to keep the stomach pH value in the therapeutically favorable range of 3–5 stable. This is achieved by a special part of the process: The more gastric acid that is present initially, the larger the amount

of acid-binding ions that are released from the crystal lattice. If more stomach acid has already been neutralized by reacting with active ingredient, the hydrotalcite releases its components slower, decreasing the solubility. The Talcid[®] product is available in two dosage forms: The liquid and chewable tablet, and it is prescribed to patients with acute or chronic gastritis. The liquid type contains 1000 mg of hydrotalcite per bag (10 mL), and the chewable tablet contains 500 mg of hydrotalcite per piece, which could neutralize gastric acid of 13 mval HCl.

Deoxyribonucleic acid (DNA)-LDH nanohybrids were proposed in 1999 by Choy's group for a most pioneering work on bio-inorganic nanomaterials [11], and later on, clearly demonstrated as the potential cellular delivery nanovectors in 2000 [12]. From then, it has opened up new research fields for their application in nanomedicine (Figure 1) [14–24]. The delivery of genes, drugs and other bioactive molecules to mammalian cells is a tremendously important research area in medicine and provides various applications for any innovative advances in the area of nanotechnology.

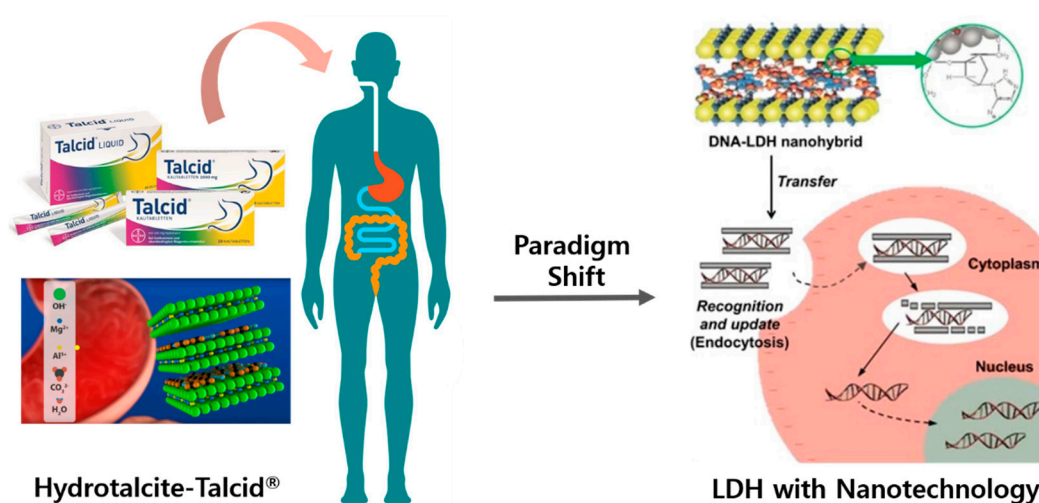


Figure 1. Schematic illustration of the paradigm shift from antacid and anti-pepsin agent, hydrotalcite-Talcid[®] to emerging cellular delivery vector, layered double hydroxide (LDH) with nanotechnology, reproduced from [3,12,17]. Images in parts 'hydrotalcite-Talcid[®]' courtesy of Bayer, Germany and Gattefosse, France.

Hydrotalcite nanohybrids have been extensively explored in biomedical fields especially for drug/gene delivery, cancer therapy and bio-imaging based on their two-dimensional (2D) layered structure, good biocompatibility and biodegradability [25–32]. LDHs comprise a unique class of 2D layered material, since they consist of positively charged brucite ($\text{Mg}[\text{OH}]_2$)-like metal hydroxide layers in which metal divalent cations are partially substituted by trivalent ones and charge-balancing interlayer anions located in the hydrated gallery between the layers. Thus, the layered structure of LDHs enables the intercalation of anionic biomolecules, such as DNA, small interfering ribonucleic acid (siRNA), anti-cancer drugs, bioactive molecules, and contrast agents into the interlayer regions mainly through electrostatic interaction.

In biomedical applications, one of the most significant factors in utilizing layered nanomaterials is biocompatibility. Among various 2D layered crystal structures, LDHs have been established as highly biocompatible, and their related nanohybrids are readily applicable for therapeutic and diagnostic uses such as anti-cancer, anti-inflammatory, antibiotic, antioxidant efficacy, and bio-imaging [33–44]. As has been well documented, efficient drug delivery carriers should not only be biocompatible to ensure safety aspects of nano delivery vehicles, but also be suitable to stabilize and protect biomolecules against harsh physical and biochemical attacks in biological environments, subsequently to deliver genes/drugs into the target-specific tissue and release them in the controlled manner. To date, as nonviral vectors, micelles, liposomes, and polymer-based nano delivery carriers have been developed as up-to-date

drug delivery systems (DDSs) [45–54], but they are inherently unstable, often leading to the pre-leakage of drugs in harsh biological environments and uncontrollable drug release *in vivo*.

The hydrotalcite nanohybrids have been considered as efficient bio-reservoirs and gene/drug delivery carriers due to their following advantages: (1) LDHs nanoparticle size, morphology, and surface properties can easily be controlled through facile synthesis and surface functionalization. Thus, the variety of possible metal compositions, for example the combination of biocompatible elements in LDH frameworks enables the lower cytotoxicity [16], doping Gd^{3+} or Mn^{2+} can confer magnetic resonance imaging (MRI) function [55,56], size or morphology control can achieve higher cellular uptake as well as more efficient intercellular delivery [57,58] and surface functionalization with specific targeting ligand for active targeting, or with fluorophore for bio-imaging [8,15,59]. (2) LDHs are stable enough to stabilize various bio-functional molecules between the positively charged metal hydroxide layers as interlayer anions with controllable gene/drug loading capacity. LDHs can protect the biomolecules by improving chemical stability and biological inertness and also enhance cellular permeability. (3) LDHs are naturally sensitive to acidic mediums because of M-OH groups, leading to bio-responsive drug delivery.

In this review, we will summarize recent developments of hydrotalcite nanohybrids for biomedical functions, including the history of the hydrotalcite-like compounds in the medical field, synthesis strategies, surface functionalization, physicochemical properties, cytotoxicity, cellular uptake mechanism, as well as their related therapeutic and diagnostic applications. The emerging research will be highlighted with related studies *in vitro* and *in vivo* (Figure 2).

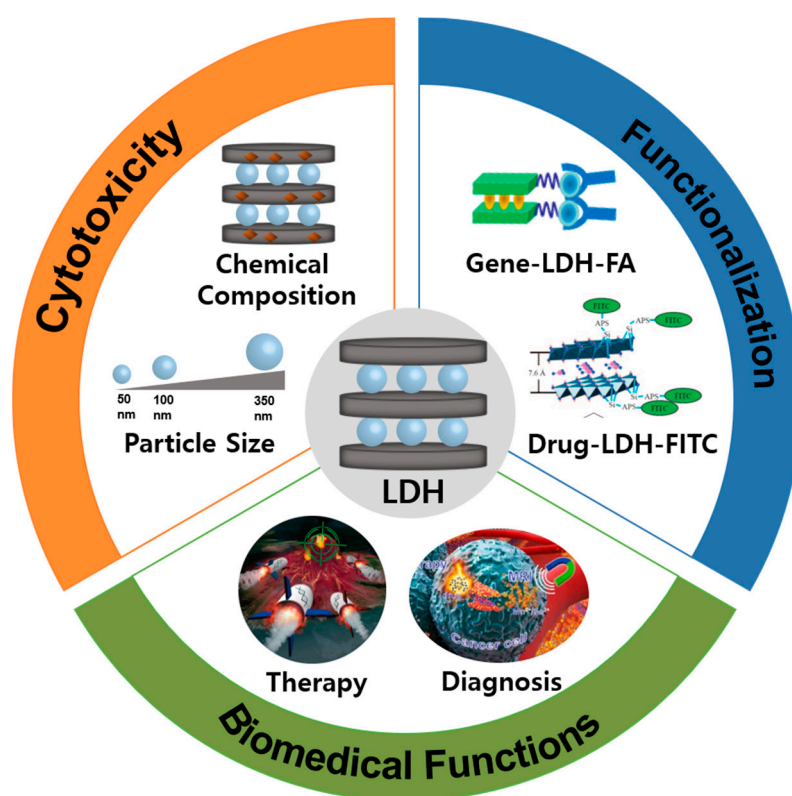


Figure 2. Overview of cytotoxicity of nanoscale hydrotalcite, functional hydrotalcite nanohybrids and their related biomedical applications, reproduced from [8,15,16].

2. Cytotoxicity of Nanoscale Hydrotalcite

Synthetic hydrotalcite is generally considered to be of good biocompatibility and low toxicity as it is able to dissolve into metal ions in acidic conditions, making it easily biodegradable in the biological system. However, the toxicological effects of LDH nanoparticles could be strongly influenced by

physicochemical properties [25,26,60]. LDHs can also be prepared with low toxicity metal elements, so their compositional versatility can be taken great advantage of, to ensure low toxicity, different from other inorganic nanoparticles which contain highly toxic or highly reactive ones. In the following section, we will describe several physicochemical parameters, such as chemical composition, particle size, and chemical stability, which can strongly affect the toxicological effects of LDH nanoparticles (Figure 3A). The cytotoxicity of nanoscale hydrotalcite has also been compared with three other inorganic nanoparticles including silica, iron oxide, and single-walled carbon nanotubes [61].

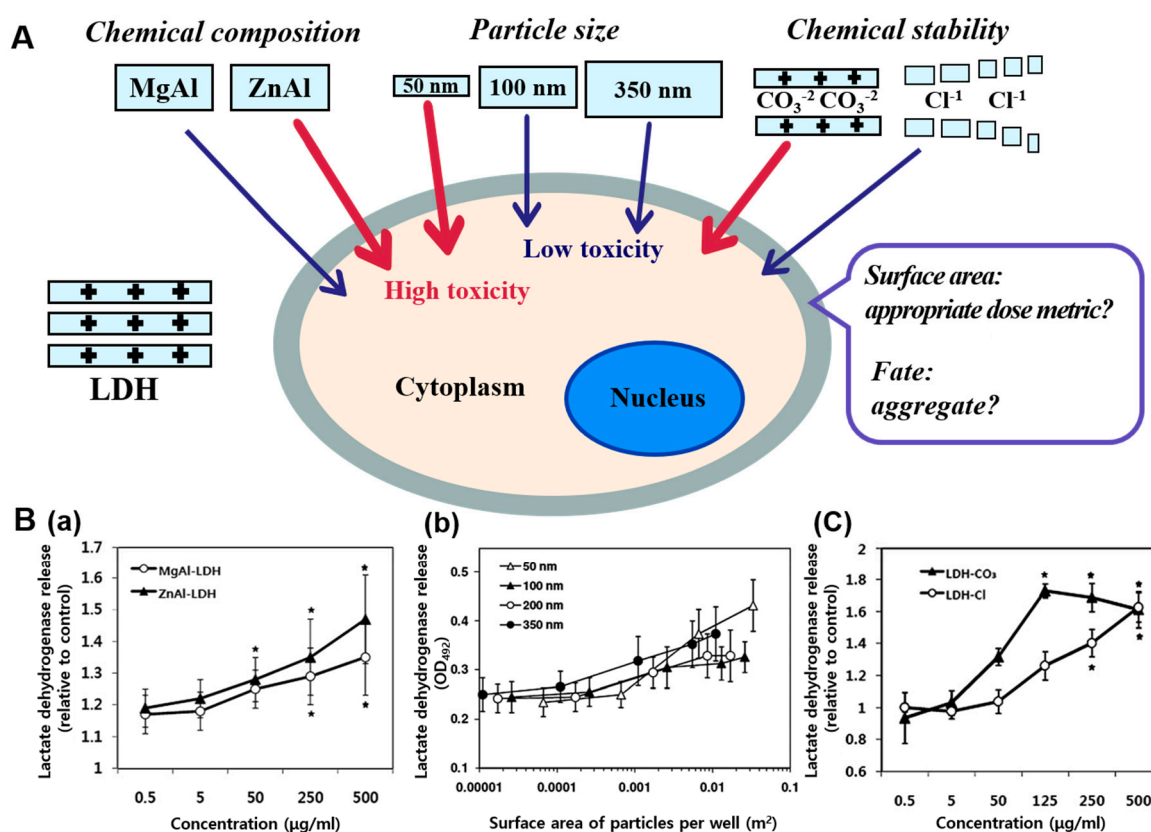


Figure 3. (A) Schematic illustration of the correlation between the chemical composition, particle size, and chemical stability of LDHs and the cytotoxicity. (B) Cytotoxicity of LDH nanoparticles with respect to (a) chemical composition, (b) particle size, and (c) chemical stability as measured by released lactate dehydrogenase levels in vitro (the blue arrows for low toxicity and the red arrows for high toxicity), reproduced from [25].

Understanding the interrelationship between the toxicity and physicochemical properties of nanoparticles is important to control and minimize their toxicity potential of manufactured nanomaterials for biomedical applications with minimized side effects. There is no doubt, that chemical composition is the most fundamental physicochemical property influencing toxicity of nanoparticles, since each element has its intrinsic chemical characteristics and reactivity in biological environments. So the nanoparticles composed of lower toxicity elements cause lower adverse effects, compared with those composed of more toxic ones. The general chemical formula of synthetic nanoscale hydrotalcite is $[M^{2+}_{1-x}M^{3+}_x(OH)_2]^{x+}(A^{m-})_{x/m} \cdot nH_2O$, where M^{2+} and M^{3+} are divalent and trivalent metal cations, respectively, and A^{m-} is the charge-balancing interlayer anion. Their chemical characteristics could be tailored from the various possible metal cation compositions and exchangeable anionic species. The divalent cations are, in general, Mg^{2+} , Zn^{2+} , Fe^{2+} , Cu^{2+} , Ca^{2+} , Ni^{2+} , and Co^{2+} and trivalent ones include Al^{3+} , Fe^{3+} , Gd^{3+} , Co^{3+} , and Ga^{3+} [2,5,28]. The variety of possible chemical compositions enables the lattice designs of various biocompatible elements in LDHs.

The cytotoxicity of LDH nanoparticles with respect to different chemical compositions (two different formulas of LDH: MgAl-LDH and ZnAl-LDH) has been evaluated in human breast cancer cell lines, because Mg^{2+}/Al^{3+} and Zn^{2+}/Al^{3+} are the most frequently used metal hydroxides combined to form positively charged sheets. MgAl-LDH and ZnAl-LDH nanoparticles with controlled particle sizes of about 200 nm were used in experiment, and the toxicity was evaluated in terms of membrane damage. According to the results, MgAl-LDH nanoparticles showed slightly less cytotoxicity than ZnAl-LDH nanoparticles, evidenced by measuring the released level of lactate dehydrogenase, a kind of the cytosolic enzyme (Figure 3B(a)). A significant cytotoxicity was assessed only at concentrations as high as 250–500 $\mu\text{g}/\text{mL}$ in both cases. A slightly higher cytotoxicity of ZnAl-LDH than MgAl-LDH could result from greater cytotoxicity of Zn^{2+} ions compared with Mg^{2+} ones. As several studies reported, zinc- and copper-based nanomaterials exhibited the most toxic effects in the cells [62]. With lattice engineering, a variety of possible compositions of LDHs can cause controllable degradation in biological environments. MgAl-LDHs are inert at pH 7.4, i.e., in the range of physiological conditions, but dissolve in weakly acidic conditions at pH 5.5–6.0 in endosomes and pH 4.5–5.0 in lysosomes.

The particle size plays an important role in cytotoxic effects. Size-dependent toxicity of LDH was assessed in cultured human lung cells. It has been demonstrated that the smallest particles with 50 nm were more toxic than larger sized particles, and LDH nanoparticles within 100–200 nm showed low cytotoxicity in terms of membrane damage, cell proliferation, and inflammation response. Four different sized MgAl-LDH nanoparticles with the sizes of 50, 100, 200, and 350 nm with a narrow size distribution were synthesized through hydrothermal reaction and their size-dependent toxicity was evaluated in A549 cells [58]. As shown in Figure 3B(b), the size-dependent cytotoxicity was more evident after 48 h exposure: The smaller the nanoparticle size is, the higher the released level of lactate dehydrogenase induced at very high concentration of 250–500 g/mL . In particular, the cytotoxicity of the smallest size of 50 nm nanoparticles considerably increased, compared with larger sized ones. This is surely related to the size-dependent cellular uptake behaviors of LDHs with four different sizes: Nanoparticles with the size of 50 nm were determined to show higher cellular uptake amount than the larger sizes of 100, 200, and 350 nm. In cultured cells, large sized particles like 350 nm may have more influence in terms of cell proliferation at high concentration (250–500 g/mL) and cause slightly higher lactate dehydrogenase release than at 100 and 200 nm. Therefore, it is concluded that LDHs with sizes of 100–200 nm are optimal *in vitro*. Size-dependent cytotoxic effects of LDH nanoparticles were also well observed in terms of inflammation response as well as membrane damage.

The structural and chemical stability of nanoparticles is significant, not only for toxicological effects, but also for delivery efficiency under systemic conditions. High stability of nanoparticles as DDSs seem to be indispensable to stably protect encapsulated bio-functional molecules from harsh physiological environments such as low pH, enzyme attack, and vascular endothelial barriers. Meanwhile, nanoparticle-based delivery carriers should easily degrade in biological systems after delivering bioactive molecules to specific target sites, in order to avoid harmful effects later that may be induced by potential bioaccumulation in the body. Cytotoxic effects with respect to chemical and structural stability was also examined in A549 cells by using different LDHs in forms of MgAl-LDH- CO_3 and MgAl-LDH-Cl, depending on interlayer anions [62]. The structural and chemical stability is affected by the interlayer anions intercalated into gallery spaces, which is stabilized mainly by electrostatic interaction. MgAl-LDH- CO_3 form with higher stability, as indicated by lower dissolution rate in simulated body fluid conditions at pH 7.4, which has been observed to have more remarkable toxicity than MgAl-LDH-Cl with lower stability with respect to released level of lactate dehydrogenase (Figure 3B(c)) and reactive oxygen species (ROS) generation. LDH- CO_3 is generally known as thermodynamically the most stable form of LDHs, thus possessing high structural and chemical stability [63]. It is concluded that low degradability of MgAl-LDH- CO_3 resulting from high stability causes elevated cytotoxicity, while biologically easily decomposed MgAl-LDH-Cl exhibits low toxicity, which is probably related to the cellular accumulation and retention time in cells.

All the results demonstrate well that toxicological effects of LDH nanoparticles can differ depending on physical and chemical parameters, providing insight into the importance of designing and controlling physicochemical properties of nanoparticles to minimize the toxicity potential.

Toxicity of LDH nanoparticles has also been evaluated by comparing with other inorganic nanoparticles such as silica, iron oxide, and single-walled carbon nanotubes that have attracted significant attention in biomedical applications. LDHs with formula $Mg_{0.68}Al_{0.32}(OH)_2(CO_3)_{0.16} \cdot 0.1H_2O$ exhibited minimal effect on cell proliferation [64]. LDH at concentration of 500 $\mu\text{g/mL}$ inhibited proliferation by 10–20% after incubation for 72 h, while iron oxide and single-walled carbon nanotube at the same concentration resulted in inhibitions of 45% and 60% in A549 cells, respectively. LDH with concentration up to 250 $\mu\text{g/mL}$ did not remarkably affect cell proliferation till 48 h, indicating its low toxicity. LDH showed relatively low toxicological effects in comparison with three other inorganic nanoparticles in lactate dehydrogenase leakage and apoptosis. The lowest lactate dehydrogenase leakage from A549 cells was also observed in LDH-treated cells, and iron oxide caused the highest release under similar conditions. LDH has induced apoptosis below 15%, even at the highest concentration at 500 $\mu\text{g/mL}$.

3. Hydrotalcite Nanohybrids for Biomedical Functions

3.1. Bio-Hydrotalcite Nanohybrids for Therapeutic Functions

Many studies have proved that synthetic hydrotalcite LDHs can intercalate and stabilize diverse bio-functional molecules, including gene, anti-cancer drugs and photosensitizer molecules to form bio-hydrotalcite nanohybrids, showing enhanced delivery efficiency and bioactivity. Bio-hydrotalcite nanohybrids as excellent intracellular delivery carriers and can be prepared through strategies, including well defined intercalation routes: Co-precipitation, ion-exchange, and exfoliation-reassembling as well as simple adsorption routes by mixing methods [28,44].

Choy et al. first reported that bio-hydrotalcite nanohybrids could be applied as potential intracellular delivery systems by means of LDH used as a nonviral vector, since LDHs are able to efficiently penetrate the cell membrane to deliver intercalated DNA and biomolecules into cells [12]. This pioneering work has opened up the whole new research field of LDHs as excellent intracellular delivery carriers. Later in 2004, methotrexate (MTX) loaded hydrotalcite nanohybrids were introduced for cancer therapy [65]. It was attempted to utilize LDH as a biocompatible nonviral vector in anti-cancer drug delivery for the first time in this work. Attractively, as-prepared MTX-LDH nanoparticles suppressed the proliferation of SaOS-2 (osteosarcoma, human) tumor cells, while showing no significant effect on the proliferation of normal cells (fibroblasts, human tendon). These comparisons indicate that drug-loaded hydrotalcite nanohybrids are ideal for anti-cancer drug design, since MTX-LDH nanohybrids are effective in killing tumor cells, but showed relatively negligible cytotoxicity in healthy cells. In 2006, intercellular uptake mechanism of LDH nanoparticles with a size of ≈ 150 nm and a hexagonal type revealed that the possibility of internalization of LDHs into cells principally via clathrin-mediated endocytosis, which is a common energy-dependent endocytic pathway in mammalian cells [13]. In vitro studies, MTX-LDH nanohybrids were prepared and labelled with fluorescein isothiocyanate (FITC) for intracellular tracing. The effectively improved delivery efficiency of MTX-LDHs is closely related to their clathrin-mediated endocytosis pathway. Such mechanism is effective only for LDHs with a nanoparticle size range of 50–200 nm. One important thing to underline is that the MTX incorporated into the LDH nanovehicle can overcome drug resistance [66], since the anti-cancer drug-LDH nanohybrid system is able to be internalized into the cancer cells via a clathrin-mediated process, which is the same as the LDH nanocarriers only.

As described in Section 2, cytotoxicity and cellular uptake mechanism of LDHs are highly size dependent. LDHs with the size of 50 nm show the highest cellular uptake, followed by an order of $50 \text{ nm} > 100\text{--}200 \text{ nm} > 350 \text{ nm}$ [58]. The related studies have continued, and in 2012, Choy et al. presented an evaluation of the intracellular trafficking mechanism and pathway of FITC-labeled LDHs

by comparing them between two different sizes of 50 and 100 nm nanoparticles [57]. It can probably maximize therapeutic effect as well as minimize the toxicity potential by controlling the particle size. Especially, 100 nm sized LDH nanoparticles are more effective for gene/drug delivery due to the manner that they could effectively escape and avoid typical endolysosomal degradation.

Recently, Park et al. developed novel bio-hydroxalcalcite nanohybrids for active tumor-targeted siRNA delivery systems [8]. In this work, the specific targeting ligand, folic acid (FA) conjugated LDH nanovectors (LDHFA) showed 3.0-fold higher suppression of tumor growth than FA-free LDH nanovector systems, which employ the enhanced permeability and retention (EPR)-based clathrin-mediated passive targeting (Figure 4A(c)). The negatively charged siRNA was self-assembled with LDHFA to form hexagonal shaped platelets with a particle size of ≈ 100 nm (Figure 4A(a)). The accumulation of siRNA in tumor tissue was also 1.2-fold higher in comparison with other organs because of improved transmission efficiency in LDHFA/siRNA treated group (Figure 4A(b)).

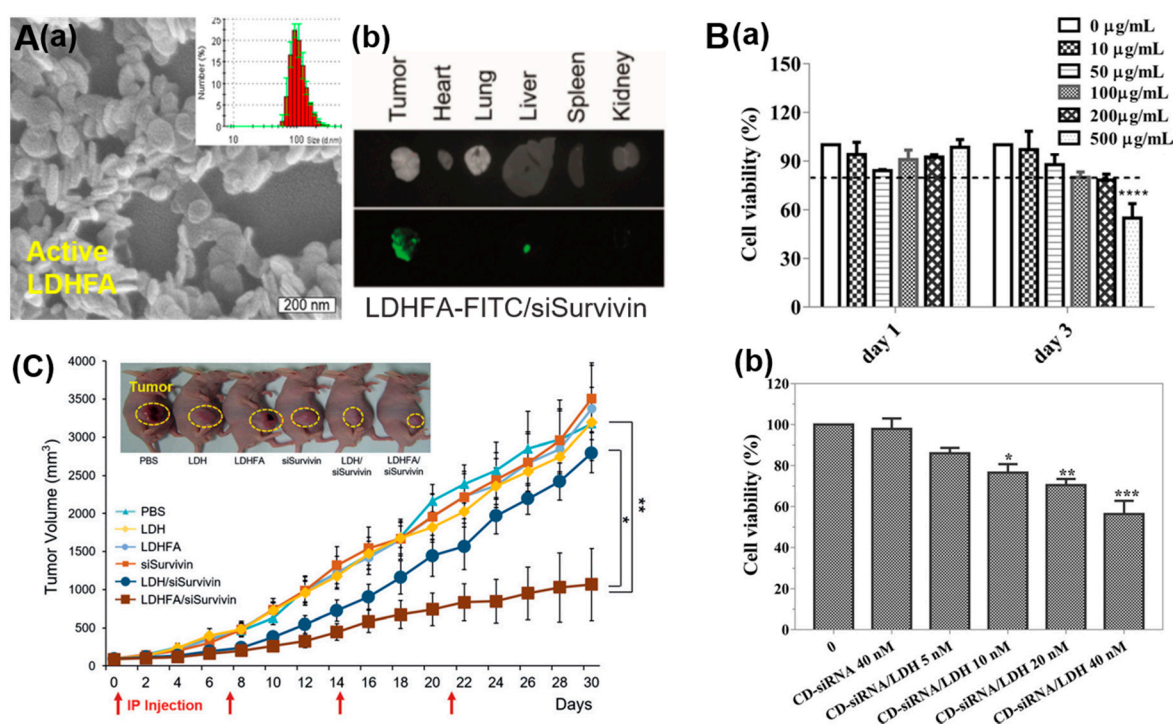


Figure 4. (A) (a) SEM image and size distributions (inset) of active LDHFA, (b) ex vivo biodistribution of the FITC-LDHFA-siSurvivin in the xenograft model: Optic (top) and fluorescence (bottom) images, (c) in vivo anti-tumor efficacy of KB tumor-bearing mice treated for 30 days via intraperitoneal injection once every 7 days (inset photo image shows the mice on 18 days post-treatment), reproduced from [8]. (B) MTT assay of the viability of N2a cells treated (a) with Mn-LDH at concentrations from 0 to 500 $\mu\text{g/mL}$, (b) with free CD-siRNA and CD-siRNA/LDHs. The siRNA:LDH mass ratio was 1:40, reproduced from reference [18].

Xu et al. reported the dually functionalized Mn-LDH of a T_1 -weighted MRI guided gene delivery system for brain cancer theranostics [18]. In this work, Mn-LDH nanovectors could accommodate siRNAs and achieve effective delivery of them to Neuro-2a (N2a) cells. As shown in Figure 4B(a), the cell viability of N2a cancer cells was higher than 80% upon after treatment with Mn-LDH at concentrations 0–200 $\mu\text{g/mL}$ after 1 and 3 days. The inhibition of N2a cancer cell proliferation was tested by methyl thiazolyltetrazolium (MTT) assay. Treatment with CD-siRNA alone did not induce any cell death at 40 nM, while treatment with CD-siRNA/Mn-LDH induced remarkably more N2a cell death (>20%) even at 10 nM, and the cell viability was further decreased to 55% at 40 nM (Figure 4B(b)).

The experiment outcomes proved the enhanced anti-cancer ability, as well as high biocompatibility with low cytotoxicity of Mn-LDH.

Besides chemo- and gene-therapy, LDHs have also been used as a photosensitizer nanovector for photodynamic and photothermal therapy [19,67,68]. Gao et al. reported types of near-infrared (NIR) activated nano-photosensitizers for singlet oxygenation and the efficient two-photon photodynamic therapy (PDT) [19]. The nano-hybrids, as two-photon photosensitizers were prepared via self-assembly of five aromatic acid guest species into LDH host. The singlet oxygen ($^1\text{O}_2$) quantum yield of nano-hybrid was up to 0.74. The good anti-cancer properties of isophthalic acid (IPA)/LDH nano-hybrids have been verified by in vitro tests with a half maximal inhibitory concentrations (IC_{50}) of 0.153 $\mu\text{g}/\text{mL}$, due to the combination of effective $^1\text{O}_2$ generation and ultrathin 2D nanosheets (Figure 5C). The biocompatibility of IPA/LDH was tested by MTT assay. The viability of cells treated with IPA/LDH was evaluated to be above 95% at concentrations as high as 500 $\mu\text{g}/\text{mL}$ (Figure 5B), indicating superior biocompatibility. IPA/LDH nanosheets were demonstrated to be ≈ 50 nm diameter (Figure 5A) and ≈ 4 nm thickness. Under 808 nm laser irradiation, IPA/LDH showed superior tissue penetration capabilities, and thus exhibited dramatically strong tumor ablation effectiveness in Hela tumors (Figure 5D).

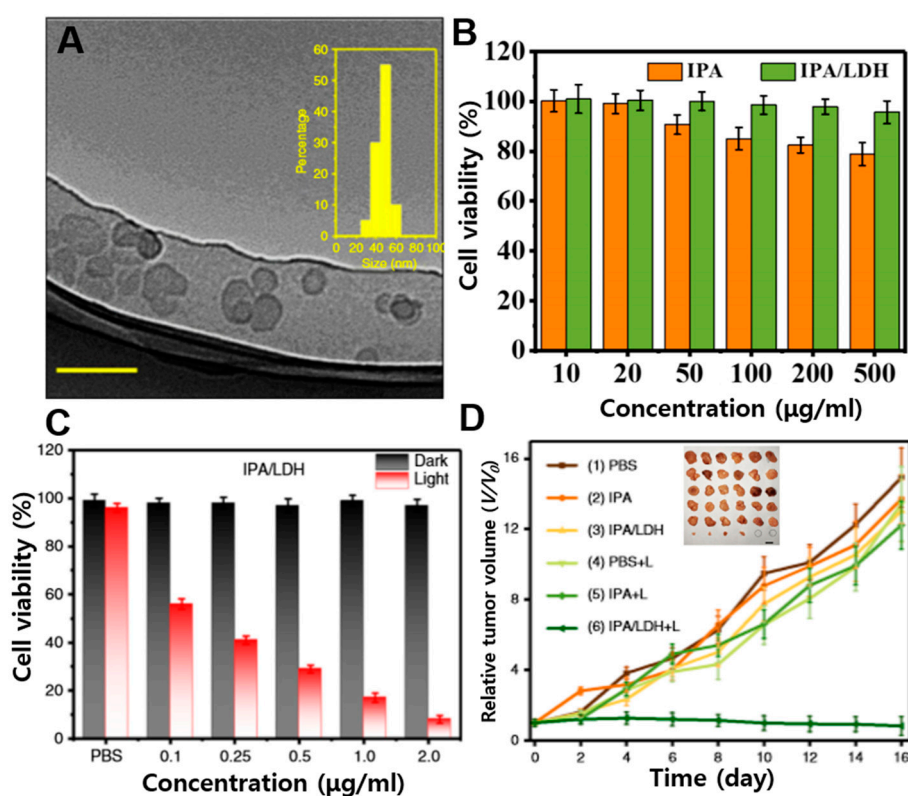


Figure 5. (A) TEM image and size distributions (inset) of IPA/LDH. (B) Cell viabilities of cells following incubation with various concentrations of IPA and IPA/LDH. (C) MTT assay of cell viabilities with and without irradiation incubated with IPA/LDH. (D) Tumor growth curves of mice with the various treatments and corresponding images of tumors taken on 16 d treatment (insert), reproduced from reference [19].

Duan et al. have developed the zinc phthalocyanine (ZnPc) (1.5%)-LDH supermolecular photosensitizers for the superior anti-cancer behavior in PDT [67]. ZnPc-LDH nano-hybrids were prepared by loading and stabilizing of ZnPc between the interlayer of LDHs, resulting in improved photostability, high $^1\text{O}_2$ production efficiency, as well as good biocompatibility. The versatile nanovehicles, co-loading of indocyanine green (ICG) and carbon dots (CDs) into the ultrathin LDHs (uLDHs), have been demonstrated for efficient photothermal therapy (PTT) and, in addition, triple-mode

imaging including photoacoustic, two-photon bio-imaging, and fluorescence [68]. The CDs/ICG-uLDHs showed efficient phototherapy properties for strong anti-cancer capability. In vitro tests with HeLa cells revealed that the viabilities of cells incubated with the CDs/ICG-uLDHs was down to 8.9%, while the groups treated with CDs and CDs-uLDHs were 82% and 78%, respectively, in presence of NIR irradiation.

3.2. Bio-Hydrotalcite Nanohybrids for Diagnostic Functions

Beyond cancer therapy, including chemo-, gene-, and photo-therapy, bio-hydrotalcite nanohybrids have also been applied to plenty of other important biomedical applications, for example bio-imaging. The structure of functional hydrotalcite nanohybrids for bio-imaging is generally three types: (1) an intercalation type, where fluorescent dyes or diethylenetriamine pentaacetic acid (Gd-DTPA), a typical example of Gd^{3+} complexes, are intercalated into the LDH interlamellar gallery; (2) a substitution type, doping metal ions, such as Mn^{2+} or Gd^{3+} in the brucite-like metal hydroxide host layer; (3) a surface functionalization type, achieved via surface chemistry using metal nanoparticles or fluorescent substances [28,69].

In many of biomedical studies, the developed materials are labelled with fluorescent dyes, such as FITC and rhodamine isothiocyanate (RITC) for intracellular tracing [15]. The fluorescent dyes are introduced into LDHs generally through intercalation route or surface functionalization. The pioneering studies of the MRI contrast agent based on LDH nanohybrids are to intercalate Gd-DTPA, a commercial contrast agent, into the gallery of LDHs to achieve the T_1 -weighted contrast agent system [70].

Li et al. have devised the novel Mn-incorporated LDH based T_1 -weighted MRI contrast agents by isomorphic substitution method, replacing partial Mg^{2+} with Mn^{2+} metal cations in Mg_3Al -LDH host layers [56]. The nano contrast agent showed pH-ultrasensitive T_1 relaxivity even at tumor microenvironment, where the pH range is very weakly acidic with pH 6.5–7.0. The satisfactory imaging performance seems to result from the unique microstructure of Mn^{2+} ions in Mn-LDH. The cytotoxicity of Mn-LDH nanoparticles at the concentration of 0–200 $\mu g/mL$ was evaluated in B16F10 cells. The cell viabilities were all above 90% during 3 d incubation, indicating that Mn-LDH nanoparticles showed a negligible effect on the cells at the concentration up to 200 $\mu g/mL$ and lower toxicity than Gd-based contrast agents.

MRI/computerized tomography (CT) bimodal probes were developed by Wang et al. in 2013 [14]. Gd-doped $MgAl$ -LDH/Au nanocomposite has been demonstrated as diagnostic agents for bimodal imagings, as well as simultaneous intracellular anti-cancer drug delivery carriers in vitro and in vivo. In this study, the disk-shaped Gd-LDH/Au nanocomposites with a size of ≈ 138 nm were functionalized by Gd^{3+} metal ions for T_1 -weighted MRI and Au nanoparticles for CT contrast agents (Figure 6A). The Gd-LDH/Au nanocomposites have showed the satisfactory in vivo and in vitro dual imaging functions (Figure 6B). The enhancements for in vivo CT and MR imagings in tumor-bearing mice were due to Gd-LDH/Au-heparin nanocomposites selectively targeting the tumor through EPR effect, which were then taken up by cancer cells. Gd-LDH/Au showed high drug loading capacity with 264 mg doxorubicine (DOX)/g carrier, effective delivery of loaded DOX into the cancer cell via endocytosis, pH-responsive release in the acidic cytoplasm and showed stronger cytotoxicity against cancer cells (Figure 6D). In addition, the cytotoxicity of the Gd-LDH/Au as carriers has been investigated in L929 cells (mouse fibroblastic cells) and HeLa cells (human cervical cancer cells). (Figure 6C). The viabilities of both cell lines were still kept above 90% even at high concentration, at 1000 mg/mL , after 24 h of incubation, indicating the negligible cytotoxicity of the carriers.

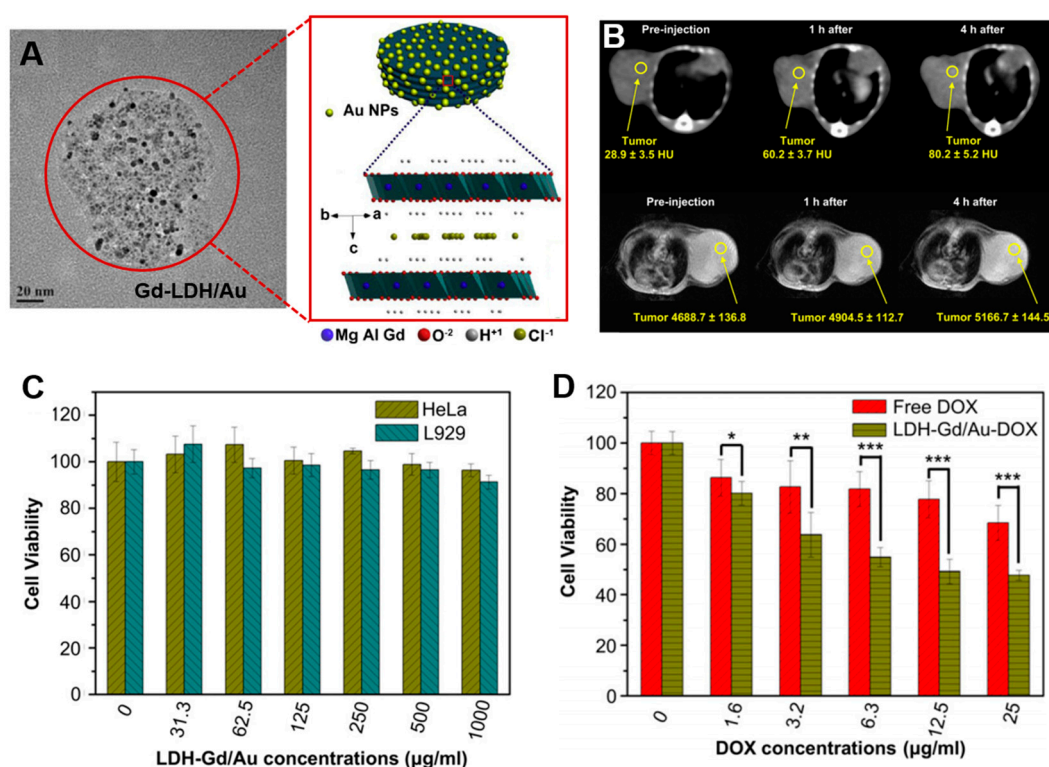


Figure 6. (A) SEM image (left) and schematic illustration (right) of LDH-Gd/Au. (B) CT (top) and MR images (bottom) of tumor after intravenous injection of Gd-LDH/Au-heparin in 4 T1 murine breast tumor-bearing mice. (C) Viabilities of L929 cell and HeLa cell incubated with LDH-Gd/Au nanocomposite without drug loading. (D) Viabilities of HeLa cell incubated with free DOX and Gd-LDH/Au-DOX at different concentrations, reproduced from [14].

As described above, research on the biomedical based on nanomaterials have exploded during the past decade and have shown the great potential for the next-generation of biomedicine technologies. However, simple delivery of one bio-functional molecule sometimes cannot satisfy the requirement of advanced biomedical applications. Taking bio-imaging as an example, multimodal imaging, in which the disadvantages could be complemented by each other and the advantages of each modality could be combined altogether synergistically, has received significant attention. In addition, synergistically integrated nano probes for combination therapies and theranostics are also explored.

4. Conclusions

Hydrotalcite has been used as antacid and anti-pepsin agent for the earliest application in medical field, but successful synthesis of hydrotalcite nanohybrids in the late 1990s has led to a paradigm shift in a whole new research field of nanoengineering, and opened up tremendously important applications in nanomedicine as emerging cellular delivery vectors. The recently emerged hydrotalcite nanohybrids for therapeutic and diagnostic applications are briefly summarized in Table 1. For biomedical applications, hydrotalcite-like anionic clay minerals, LDH-based nanohybrids offer many advantages. (1) LDHs nanoparticle size, morphology, and surface properties can easily be controlled through facile synthesis and surface functionalization. (2) LDHs are stable enough to stabilize various bio-functional molecules between the positively charged metal hydroxide layers as interlayer anions with controllable gene/drug loading capacity. (3) LDHs are naturally sensitive to acidic medium because of M-OH groups, leading to bio-responsive drug delivery. (4) The flexibility of manipulation on the nanometer scale of LDH-based nanocomposites is a superior advantage. This research field should be expanded, especially synergistic integration with various materials which can enhance the performance of LDH or complement the limitation of LDH nanostructures [71–73].

Table 1. A brief summary of hydrotalcite nanohybrids with biomedical functions.

LDH Host	Synthetic Method	Particle Size [nm]	Bio-Functional Molecules	Cell Line and Animal Model	Application	Refs.
MgAl	Ion-exchange	-	DNA, adenosine triphosphate, FITC	NIH3T3 cells, HL-60 cells	Gene-therapy, fluorescence imaging	[12]
MgAl	Ion-exchange	150	MTX, FITC	MNNG cells, HOS cells	Chemo-therapy, fluorescence imaging	[13]
MgAl	Ion-exchange	-	MTX,	Fibroblast, SaOS-2 cells	Chemo-therapy	[65]
MgAl	Co-precipitation	100	MTX	HOS cells, HOS/Mtx cells	Chemo-therapy	[66]
MgAl	Co-precipitation, silane coupling	100	siRNA, FITC	KB cells, A549 cells, xenograft mice model bearing KB tumor	Gene-therapy, fluorescence imaging	[8]
MnAl	Co-precipitation, self-assembly	125	siRNA, Mn ²⁺	Neuro-2a cells	Gene-therapy, MRI	[18]
ZnAl	Co-precipitation	50	Isophthalic acid (IPA), Cy5.5	Hela cells, Balb/c nude mice bearing Hela tumor	Singlet oxygenation, PDT, NIR fluorescence imaging	[19]
MgAl	Co-precipitation	120	ZnPc	HepG2 cells, male Balb/c mice bearing HepG2 tumor	Singlet oxygenation, PDT	[67]
MgAl	self-assembly	20–50	CDs, ICG	Hela cells, HepG-2 cells, male Balb/c mice bearing Hela tumor	PTT, fluorescence imaging, photoacoustic imaging, two-photon imaging	[68]
ZnAl	Co-precipitation	120	Gd-DTPA	-	MRI	[70]
MnMgAl	Co-precipitation, isomorphic substitution	20–80	Mn ²⁺	B16F10 cells (mouse melanoma skin cancer cell line), mouse bearing the melanoma tumor	MRI	[56]
GdMgAl	Co-precipitation, self-assembly	138	DOX, Gd ³⁺ , Au NPs	L929 cells, HeLa cells, mice bearing 4T1 murine breast tumor	Chemo-therapy, MRI, CT	[14]

Here, we have described the interrelationship between the cytotoxicity and physicochemical properties of LDH nanoparticles. LDHs can be synthesized with biocompatible metal elements and easily degrade in biological systems due to their pH-dependent solubility. LDHs with sizes of 100–200 nm are optimal in vitro and biologically easily decomposed MgAl-LDH-Cl exhibits low toxicity. Understanding the interrelationship between toxicological effects and physicochemical properties could provide insight into the importance of designing and controlling physical and chemical parameters of nanoparticles to minimize the toxicity potential. The emerging strategies for biomedical applications, including chemo-, gene-, photo-therapy and bio-imaging, have been highlighted with related studies in vitro and in vivo, as well as the cytotoxicity effect. With further improvement in cellular delivery vector techniques, hydrotalcite nanohybrids-supported DDSs are expected to contribute to extensive clinical applications in the near future.

Acknowledgments: This work was supported by the National Research Foundation of Korea (NRF) grant, funded by the Korean government (MSIT) (No. NRF-2019R1G1A1006582).

Conflicts of Interest: The authors declare no conflict of interest.

References

- Evans, D.G.; Slade, R.C.T. Structural Aspects of Layered Double Hydroxides. *Struct. Bond.* **2006**, *119*, 1–87.
- Simoneau, G. Absence of rebound effect with calcium carbonate. *Eur. J. Drug Metab. Pharmacokinet.* **1996**, *21*, 351–357. [[CrossRef](#)] [[PubMed](#)]

3. Hydrotalcite-Talcid®. Available online: <https://www.talcid.de/talcid-produkte/hydrotalcit/> (accessed on 1 November 2018).
4. Park, D.H.; Hwang, S.J.; Oh, J.M.; Yang, J.H.; Choy, J.H. Polymer–inorganic supramolecular nanohybrids for red, white, green, and blue applications. *Prog. Polym. Sci.* **2013**, *38*, 1442–1486. [[CrossRef](#)]
5. Oh, J.M.; Park, D.H.; Choi, S.J.; Choy, J.H. LDH nanocontainers as bio-reservoirs and drug delivery carriers. *Recent Pat. Nanotech.* **2012**, *6*, 200–217. [[CrossRef](#)] [[PubMed](#)]
6. Mishra, G.; Dash, B.; Pandey, S. Layered double hydroxides: A brief review from fundamentals to application as evolving biomaterials. *Appl. Clay Sci.* **2018**, *153*, 172–186. [[CrossRef](#)]
7. Oh, J.M.; Park, D.H.; Choy, J.H. Integrated bio-inorganic hybrid systems for nano-forensics. *Chem. Soc. Rev.* **2011**, *40*, 583–595. [[CrossRef](#)]
8. Park, D.H.; Cho, J.; Kwon, O.J.; Yun, C.O.; Choy, J.H. Biodegradable Inorganic Nanovector: Passive versus Active Tumor Targeting in siRNA Transportation. *Angew. Chem. Int. Ed.* **2016**, *55*, 4582–4586. [[CrossRef](#)]
9. Park, D.H.; Kim, J.E.; Oh, J.M.; Shul, Y.G.; Choy, J.H. DNA Core@Inorganic Shell. *J. Am. Chem. Soc.* **2010**, *132*, 16735–16736. [[CrossRef](#)]
10. Ward, M.D. Plastic sandwiches à la carte. *Nature* **2000**, *405*, 293–294. [[CrossRef](#)]
11. Choy, J.H.; Kwak, S.Y.; Park, J.S.; Jeong, Y.J.; Portier, J. Intercalative nanohybrids of nucleoside monophosphates and DNA in layered metal hydroxide. *J. Am. Chem. Soc.* **1999**, *121*, 1399–1400. [[CrossRef](#)]
12. Choy, J.H.; Kwak, S.Y.; Jeong, Y.J.; Park, J.S. Inorganic Layered Double Hydroxides as Nonviral Vectors. *Angew. Chem.* **2000**, *39*, 4041–4045. [[CrossRef](#)]
13. Oh, J.M.; Choi, S.J.; Kim, S.T.; Choy, J.H. Cellular Uptake Mechanism of an Inorganic Nanovehicle and Its Drug Conjugates: Enhanced Efficacy Due To Clathrin-Mediated Endocytosis. *Bioconjugate Chem.* **2006**, *17*, 1411–1417. [[CrossRef](#)] [[PubMed](#)]
14. Wang, L.; Xing, H.; Zhang, S.; Ren, Q.; Pan, L.; Zhang, K.; Bu, W.; Zheng, X.; Zhou, L.; Peng, W.; et al. A Gd-doped Mg-Al-LDH/Au nanocomposite for CT/MR bimodal imagings and simultaneous drug delivery. *Biomaterials* **2013**, *34*, 3390–3401. [[CrossRef](#)] [[PubMed](#)]
15. Oh, J.M.; Choi, S.J.; Lee, G.E.; Kim, J.E.; Choy, J.H. Inorganic Metal Hydroxide Nanoparticles for Targeted Cellular Uptake Through Clathrin-Mediated Endocytosis. *Chem. Asian J.* **2009**, *4*, 67–73. [[CrossRef](#)]
16. Huang, G.; Zhang, K.L.; Chen, S.; Li, S.H.; Wang, L.L.; Wang, L.P.; Liu, R.; Gao, J.; Yang, H.H. Manganese-iron layered double hydroxide: A theranostic nanoplatform with pH-responsive MRI contrast enhancement and drug release. *J. Mater. Chem. B* **2017**, *5*, 3629–3633. [[CrossRef](#)]
17. SEDDS for Oral Peptide Delivery: Gattefossé Insight. Available online: <https://www.in-pharmatechnologist.com/> (accessed on 22 November 2017).
18. Zuo, H.; Chen, W.; Li, B.; Xu, K.; Cooper, H.; Gu, Z.; Xu, Z.P. MnAl Layered Double Hydroxide Nanoparticles as a Dual-Functional Platform for Magnetic Resonance Imaging and siRNA Delivery. *Chem. Eur. J.* **2017**, *23*, 14299–14306. [[CrossRef](#)]
19. Gao, R.; Mei, X.; Yan, D.; Liang, R.; Wei, M. Nano-photosensitizer based on layered double hydroxide and isophthalic acid for singlet oxygenation and photodynamic therapy. *Nat. Commun.* **2018**, *9*, 2798. [[CrossRef](#)]
20. Ladewig, K.; Xu, Z.P.; Lu, G.Q. Layered double hydroxide nanoparticles in gene and drug delivery. *Expert Opin. Drug Deliv.* **2009**, *6*, 907–922. [[CrossRef](#)]
21. Liang, R.; Wei, M.; Evans, D.G.; Duan, X. Inorganic nanomaterials for bioimaging, targeted drug delivery and therapeutics. *Chem. Commun.* **2014**, *50*, 14071–14081. [[CrossRef](#)]
22. Hermansson, L. A Review of Nanostructured Ca-aluminate Based Biomaterials within Odontology and Orthopedics. *J. Korean Ceram. Soc.* **2018**, *55*, 95–107. [[CrossRef](#)]
23. Weissleder, R. Molecular Imaging in Cancer. *Science* **2006**, *312*, 1168–1171. [[CrossRef](#)] [[PubMed](#)]
24. Eslami, H.; Tahiri, M.; Moztafzadeh, F.; Bader, R.; Tayebi, L. Nanostructured Hydroxyapatite for Biomedical Applications: From Powder to Bioceramic. *J. Korean Ceram. Soc.* **2018**, *55*, 597–607. [[CrossRef](#)]
25. Choi, S.J.; Choy, J.H. Effect of physico-chemical parameters on the toxicity of inorganic nanoparticles. *J. Mater. Chem.* **2011**, *21*, 5547–5554. [[CrossRef](#)]
26. Choi, S.J.; Choy, J.H. Layered double hydroxide nanoparticles as target-specific delivery carriers: Uptake mechanism and toxicity. *Nanomedicine* **2011**, *6*, 803–814. [[CrossRef](#)] [[PubMed](#)]
27. Rives, V.; Arco, M.; Martín, C. Intercalation of drugs in layered double hydroxides and their controlled release: A review. *Appl. Clay Sci.* **2014**, *88*, 239–269. [[CrossRef](#)]

28. Park, D.H.; Choi, G.; Choy, J.H. Bio-Layered Double Hydroxides Nanohybrids for Theranostics Applications. In *Photofunctional Layered Materials; Structure and Bonding*; Springer: Cham, Switzerland, 2015; Volume 166, pp. 137–175.
29. Xie, W.S.; Guo, Z.H.; Cao, Z.B.; Gao, Q.; Wang, D.; Boyer, C.; Kallavaris, M.; Sun, X.D.; Wang, X.M.; Zhao, L.Y.; et al. Manganese-based magnetic layered double hydroxide nanoparticle: A pH-sensitive and concurrently enhanced T_1/T_2 -weighted dual-mode magnetic resonance imaging contrast agent for accurate cancer diagnosis. *ACS Biomater. Sci. Eng.* **2019**, *5*, 2555–2562. [[CrossRef](#)]
30. Jung, Y.; Ji, E.; Capasso, A.; Lee, G.H. Recent Progresses in the Growth of Two-dimensional Transition Metal Dichalcogenides. *J. Korean Ceram. Soc.* **2019**, *56*, 24–36. [[CrossRef](#)]
31. Hakeem, A.; Zhan, G.T.; Xu, Q.B.; Yong, T.Y.; Gan, L.; Yang, X.L. Facile synthesis of pH-responsive doxorubicin-loaded layered double hydroxide for efficient cancer therapy. *J. Mater. Chem. B* **2018**, *6*, 5768–5774. [[CrossRef](#)]
32. Rives, V.; Arco, M.; Martín, C. Layered double hydroxides as drug carriers and for controlled release of non-steroidal antiinflammatory drugs (NSAIDs): A review. *J. Control. Release* **2013**, *169*, 28–39. [[CrossRef](#)]
33. Ribeiro, L.N.M.; Alcantara, A.C.S.; Darder, M.; Aranda, P.; Araújo-Moreira, F.M.; Ruiz-Hitzky, E. Pectin-coated chitosan-LDH bionanocomposite beads as potential systems for colon-targeted drug delivery. *Int. J. Pharm.* **2014**, *463*, 1–9. [[CrossRef](#)]
34. Ryu, S.J.; Jung, H.; Oh, J.M.; Lee, J.K.; Choy, J.H. Layered double hydroxide as novel antibacterial drug delivery system. *J. Phys. Chem. Solids* **2010**, *71*, 685–688. [[CrossRef](#)]
35. Yang, J.H.; Lee, S.Y.; Yang, S.; Park, K.C.; Choy, J.H. Efficient Transdermal Penetration and Improved Stability of L-Ascorbic Acid Encapsulated in an Inorganic Nanocapsule. *Bull. Korean Chem. Soc.* **2003**, *24*, 499–503.
36. Son, Y.J.; Lee, I.C.; Jo, H.H.; Chung, T.J.; Oh, K.S. Setting Behavior and Drug Release from Brushite Bone Cement prepared with Granulated Hydroxyapatite and β -Tricalcium Phosphate. *J. Korean Ceram. Soc.* **2019**, *56*, 56–64. [[CrossRef](#)]
37. Jin, W.J.; Park, D.H. Info-Convergence Ceramic Nanosystems. *J. Korean Ceram. Soc.* **2019**, *56*, 421–434. [[CrossRef](#)]
38. Zhao, X.; Yang, C.X.; Chen, L.G.; Yan, X.P. Dual-stimuli responsive and reversibly activatable theranostic nanoprobe for precision tumor-targeting and fluorescence-guided photothermal therapy. *Nat. Commun.* **2017**, *8*, 1–9. [[CrossRef](#)]
39. Choi, G.; Jeon, I.R.; Piao, H.; Choy, J.H. Highly Condensed Boron Cage Cluster Anions in 2D Carrier and Its Enhanced Antitumor Efficiency for Boron Neutron Capture Therapy. *Adv. Funct. Mater.* **2017**, *28*, 1704470. [[CrossRef](#)]
40. Wang, D.; Ge, N.; Yang, T.; Peng, F.; Qiao, Y.; Li, Q.; Liu, X. NIR-Triggered Crystal Phase Transformation of NiTi-Layered Double Hydroxides Films for Localized Chemothermal Tumor Therapy. *Adv. Sci.* **2018**, *5*, 1700782. [[CrossRef](#)]
41. Mei, X.; Liang, R.; Peng, L.; Hu, T.; Wei, M. Layered double hydroxide bio-composites toward excellent systematic anticancer therapy. *J. Mater. Chem. B* **2017**, *5*, 3212–3216. [[CrossRef](#)]
42. Wang, N.; Wang, Z.; Xu, Z.; Chen, X.; Zhu, G. A Cisplatin-Loaded Immunochemotherapeutic Nanohybrid Bearing Immune Checkpoint Inhibitors for Enhanced Cervical Cancer Therapy. *Angew. Chem.* **2018**, *130*, 3484–3488. [[CrossRef](#)]
43. Taviot-Guého, C.; Prévot, V.; Forano, C.; Renaudin, G.; Mousty, C.; Leroux, F. Tailoring Hybrid Layered Double Hydroxides for the Development of Innovative Applications. *Adv. Funct. Mater.* **2017**, *28*, 1703868. [[CrossRef](#)]
44. Choi, G.; Eom, S.; Vinu, A.; Choy, J.H. 2D Nanostructured Metal Hydroxides with Gene Delivery and Theranostic Functions; A Comprehensive Review. *Chem. Rec.* **2018**, *18*, 1–22. [[CrossRef](#)] [[PubMed](#)]
45. Misra, A.; Jain, S.; Kishore, D.; Dave, V.; Reddy, K.R.; Sadhu, V.; Dwivedi, J.; Sharma, S. A facile one pot synthesis of novel pyrimidine derivatives of 1, 5-benzodiazepines via domino reaction and their antibacterial evaluation. *J. Microbiol. Methods* **2019**, *163*, 105648. [[CrossRef](#)] [[PubMed](#)]
46. Sharma, M.; Deohra, A.; Reddy, K.R.; Sadhu, V. Biocompatible in-situ gelling polymer hydrogels for treating ocular infection. In *Methods in Microbiology; Nanotechnology*; Elsevier: Amsterdam, The Netherlands, 2019; Volume 46, pp. 93–114.

47. Gullaa, S.; Lomadab, D.; Srikanthc, V.V.; Shankard, M.V.; Reddye, K.R.; Sonif, S.; Reddy, M.C. Recent Advances in Nanoparticles-Based Strategies for Cancer Therapeutics and Antibacterial Applications. In *Methods in Microbiology; Nanotechnology*; Elsevier: Amsterdam, The Netherlands, 2019; Volume 46, pp. 255–293.
48. Paliwal, S.; Tilak, A.; Sharma, J.; Dave, V.; Sharma, S.; Verma, K.; Tak, K.; Reddy, K.R.; Sadhu, V. Flurbiprofen-loaded ethanolic liposome particles for biomedical applications. *J. Microbiol. Methods* **2019**, *161*, 18–27. [[CrossRef](#)] [[PubMed](#)]
49. Dave, V.; Tak, K.; Sohgaure, A.; Gupta, A.; Sadhu, V.; Reddy, K.R. Lipid-polymer hybrid nanoparticles: Synthesis strategies and biomedical applications. *J. Microbiol. Methods* **2019**, *160*, 130–142. [[CrossRef](#)] [[PubMed](#)]
50. Xia, N.; Li, N.; Rao, W.; Yu, J.; Wu, Q.; Tan, L.; Li, H.; Gou, L.; Liang, P.; Li, L.; et al. Multifunctional and flexible ZrO₂-coated EGaIn nanoparticles for photothermal therapy. *Nanoscale* **2019**, *11*, 10183–10189. [[CrossRef](#)]
51. Patil, S.B.; Inamdar, S.Z.; Reddy, K.R.; Raghu, A.V.; Soni, S.K.; Kulkarni, R.V. Novel biocompatible poly (acrylamide)-grafted-dextran hydrogels: Synthesis, characterization and biomedical applications. *J. Microbiol. Methods* **2019**, *159*, 200–210. [[CrossRef](#)]
52. Boppana, R.; Raut, S.Y.; Mohan, G.K.; Sa, B.; Mutalik, S.; Reddy, K.R.; Das, K.K.; Biradar, M.S.; Kulkarni, R.V. Novel pH-sensitive interpenetrated network polyspheres of polyacrylamide-g-locust bean gum and sodium alginate for intestinal targeting of ketoprofen: In vitro and in vivo evaluation. *Colloids Surf. B Biointerfaces* **2019**, *180*, 362–370. [[CrossRef](#)]
53. Sur, S.; Rathore, A.; Dave, V.; Reddy, K.R.; Chouhan, R.S.; Sadhu, V. Recent developments in functionalized polymer nanoparticles for efficient drug delivery system. *Nano-Struct. Nano-Obj.* **2019**, *20*, 100397. [[CrossRef](#)]
54. Dave, V.; Gupta, A.; Singh, P.; Gupta, C.; Sadhu, V.; Reddy, K.R. Synthesis and characterization of celecoxib loaded PEGylated liposome nanoparticles for biomedical applications. *Nano-Struct. Nano-Obj.* **2019**, *18*, 100288. [[CrossRef](#)]
55. Peng, L.; Mei, X.; He, J.; Xu, J.; Zhang, W.; Liang, R.; Wei, M.; Evans, D.G.; Duan, X. Monolayer Nanosheets with an Extremely High Drug Loading toward Controlled Delivery and Cancer Theranostics. *Adv. Mater.* **2018**, *30*, 1707389. [[CrossRef](#)]
56. Li, B.; Gu, Z.; Kurniawan, N.; Chen, W.; Xu, Z.P. Manganese-Based Layered Double Hydroxide Nanoparticles as a T₁-MRI Contrast Agent with Ultrasensitive pH Response and High Relaxivity. *Adv. Mater.* **2017**, *29*, 1700373. [[CrossRef](#)]
57. Chung, H.E.; Park, D.H.; Choy, J.H.; Choi, S.J. Intracellular trafficking pathway of layered double hydroxide nanoparticles in human cells: Size-dependent cellular delivery. *Appl. Clay Sci.* **2012**, *65–66*, 24–30. [[CrossRef](#)]
58. Choi, S.J.; Oh, J.M.; Choy, J.H. Safety Aspect of Inorganic Layered Nanoparticles: Size-Dependency In Vitro and In Vivo. *J. Nanosci. Nanotechnol.* **2008**, *8*, 5297–5301. [[CrossRef](#)] [[PubMed](#)]
59. Chen, W.Y.; Zuo, H.L.; Zhang, E.Q.; Li, L.; Henrich-Noack, P.; Cooper, H.M.; Qian, Y.J.; Xu, Z.P. Brain targeting delivery facilitated by ligand-functionalized layered double hydroxide nanoparticles. *ACS Appl. Mater. Interfaces* **2017**, *24*, 20326–20333. [[CrossRef](#)] [[PubMed](#)]
60. Park, J.; Na, H.; Choi, S.C.; Kim, H.J. Biocompatibility of 13–93 Bioactive Glass-SiC Fabric Composites. *J. Korean Ceram. Soc.* **2019**, *56*, 205–210. [[CrossRef](#)]
61. Kim, D.K.; Lee, J.W. Synthesis of Non-hydrate Iron Oleate for Eco-friendly Production of Monodispersed Iron Oxide Nanoparticles. *J. Korean Ceram. Soc.* **2018**, *55*, 625–634. [[CrossRef](#)]
62. Lanone, S.; Rogerieux, F.; Geys, J.; Dupont, A.; Maillot-Marechal, E.; Boczkowski, J.; Lacroix, G.; Hoet, P. Comparative toxicity of 24 manufactured nanoparticles in human alveolar epithelial and macrophage cell lines. *Part. Fibre Toxicol.* **2009**, *6*, 14. [[CrossRef](#)] [[PubMed](#)]
63. Baek, M.; Kim, I.S.; Yu, J.; Chung, H.E.; Choy, J.H.; Choi, S.J. Effect of Different Forms of Anionic Nanoclays on Cytotoxicity. *J. Nanosci. Nanotechnol.* **2011**, *11*, 1803–1806. [[CrossRef](#)]
64. Choi, S.J.; Oh, J.M.; Choy, J.H. Toxicological effects of inorganic nanoparticles on human lung cancer A549 cells. *J. Inorg. Biochem.* **2009**, *103*, 463–471. [[CrossRef](#)]
65. Choy, J.H.; Jung, J.S.; Oh, J.M.; Park, M.; Jeong, J.Y.; Kang, Y.K.; Han, O.J. Layered double hydroxide as an efficient drug reservoir for folate derivatives. *Biomaterials* **2004**, *25*, 3059–3064. [[CrossRef](#)]
66. Choi, S.J.; Choi, G.E.; Oh, J.M.; Oh, Y.J.; Park, M.C.; Choy, J.H. Anticancer drug encapsulated in inorganic lattice can overcome drug resistance. *J. Mater. Chem.* **2010**, *20*, 9463–9469. [[CrossRef](#)]

67. Liang, R.; Tian, R.; Ma, L.; Zhang, L.; Hu, Y.; Wang, J.; Wei, M.; Yan, D.; Evans, D.G.; Duan, X. A Supramolecular Photosensitizer with Excellent Anticancer Performance in Photodynamic Therapy. *Adv. Funct. Mater.* **2014**, *24*, 3144–3151. [[CrossRef](#)]
68. Weng, Y.; Guan, S.; Lu, H.; Meng, X.; Kaassis, A.Y.; Ren, X.; Qu, X.; Sun, C.; Xie, Z.; Zhou, S. Confinement of carbon dots localizing to the ultrathin layered double hydroxides toward simultaneous triple-mode bioimaging and photothermal therapy. *Talanta* **2018**, *184*, 50–57. [[CrossRef](#)] [[PubMed](#)]
69. Kim, J.; Lee, E.; Hong, Y.; Kim, B.; Ku, M.; Heo, D.; Choi, J.; Na, J.; You, J.; Haam, S.; et al. Self-doped conjugated polymeric nanoassembly by simplified process for optical cancer theragnosis. *Adv. Funct. Mater.* **2015**, *25*, 2260–2269. [[CrossRef](#)]
70. Kim, S.Y.; Oh, J.M.; Lee, J.S.; Kim, T.J.; Choy, J.H. Gadolinium (III) Diethylenetriamine Pentaacetic Acid/Layered Double Hydroxide Nanohybrid as Novel T₁-Magnetic Resonant Nanoparticles. *J. Nanosci. Nanotechnol.* **2008**, *8*, 5181–5184. [[CrossRef](#)]
71. Yan, L.; Gonca, S.; Zhu, G.; Zhang, W.; Chen, X. Layered double hydroxide nanostructures and nanocomposites for biomedical applications. *J. Mater. Chem. B.* **2019**, *7*, 5583–5601. [[CrossRef](#)]
72. Costantino, U.; Nocchetti, M.; Tammaro, L.; Vittoria, V. Modified hydrotalcite-like compounds as active fillers of biodegradable polymers for drug release and food packaging applications. *Recent Pat. Nanotechnol.* **2012**, *6*, 218–230. [[CrossRef](#)]
73. Toson, V.; Conterposito, E.; Palin, L.; Boccaleri, E.; Milanesio, M.; Gianotti, V. Facile intercalation of organic molecules into hydrotalcites by liquid assisted grinding: Yield optimization by a chemometric approach. *Cryst. Growth Des.* **2015**, *15*, 5368–5374. [[CrossRef](#)]



© 2020 by the authors. Licensee MDPI, Basel, Switzerland. This article is an open access article distributed under the terms and conditions of the Creative Commons Attribution (CC BY) license (<http://creativecommons.org/licenses/by/4.0/>).